pA_2 value is defined as the negative logarithm of the molar concentration of the test compound that will cause a shift of a factor of 2 toward higher concentration in the Ca^{2+} concentration–response curve.

Blood Pressure and Heart Rate in Spontaneously Hypertensive Rats. Experiments were carried out in spontaneously hypertensive male rats (Okamoto strain), which were at least 16 weeks old. An arterial catheter (Clay Adams, PE-50) was implanted into an abdominal aorta via a femoral artery under ether anesthesia. Conscious blood pressure was measured directly by the arterial catherter that was connected to a pressure transducer (Nihon Koden, TR-200T). Heart rate was measured by a pulse rate tachometer (Nihon Koden, AT-601G).

Methacholine-Induced ST Elevation in Rats. Male Sprague-Dawley rats, weighing about 500 g, were anesthetized with sodium pentobarbital (60 mg/kg ip). For bolus injection of methacholine into the ostia of the left and right coronary arteries, an arterial cannula was introduced through the exposed right carotid artery down closely to the aortic valve. Methacholine solutions (8 μg/kg) were administered ia into the aorta by means of microsyringes before, 0.5 min and every 5 min (until abolish of methacholine-induced ST elevation) after test drug administration. Test compound solutions were intravenously administered into the femoral vein. Recording of ECG, sensitivity of ECG, and amplitude of ST segment were achieved by the same method as used with the vasopressin-induced ST depression assay. Values are represented as mean ± SE. The difference of paired mean values was analyzed by the Student's *t*-test and judged to be significant when *p* values were less than 0.05.

Vasopressin-Induced ST Depression in Rats. Male rats of the Donryu strain, weighing 150–220 g, were anesthetized with sodium pentobarbital (60 mg/kg ip). The test compounds suspended in 0.5% tragacanth solution were administered orally 60 min before intravenous administration of vasopressin (0.2 IU/kg). After 60 min, using the method of Hiramatsu et al.,[7a] myocardial hypoxia was produced with vasopressin, which was administered through a cannula in the femoral vein. The electrocardiogram (ECG) of the standard limb lead II was recorded. ST segment depression after vasopressin was measured, as previously described by Hatano et al.[7b] The amplitude of the ST segment was measured at intervals of 30 s for 5 min after administration of vasopressin in each rat.

Calcium Influx in Rat Aorta. Thoracic aorta was cut open longitudinally and a segment weighing about 5–10 mg was used for the experiments. The artery strips were incubated for 5 min in ^{45}Ca (0.8 μCi of ^{45}Ca/mL) containing physiological solution (mM: NaCl 136.9, KCl 5.4, $MgSO_4$ 1.0, $CaCl_2$ 1.5, $NaHCO_3$ 23.8, glucose 5.5). Test compounds were added 30 min prior to and during the ^{45}Ca incubation period. After incubation with ^{45}Ca, the strips were washed for 60 min at 4 °C in the La-substituted solution containing 73.8 mM $LaCl_3$, 5.5 mM glucose and 24 mM tris(hydroxymethyl)aminomethane. After the La-wash period, tissues were placed in scintillation vials and dissolved in soluene solution at 40 °C. The scintillation mixture was added to toluene scintillation solution (mM: dimethyl-POPOP 0.25, PPO 22.6, acetic acid 143), and the radioactivity was counted in a liquid scintillation counter (Packard Model 1460 CD). The results of each determination were convered to the apparent tissue content of

$$^{45}Ca\ (\text{mmol/kg of wet wt}) = \frac{\text{dpm in muscle}}{\text{wet wt (kg)}} \times \frac{\text{nmol of Ca/L of medium}}{\text{dpm/L of medium}}$$

IC_{50} values were estimated from concentration–effect curves.

High Potassium Induced Contraction in Rat Aorta. Muscle tension was recorded isometrically with a force-displacement transducer (Nihon Koden TB-611T). Isosmotic 80.0 mmol K-induced contractions in rat aorta were used for standard K-induced contractions. The test compounds were added 30 min before measurement. The concentrations of the test compounds required to induce a 50% inhibition of contraction (IC_{50}) were calculated from the cumulative concentration–inhibition curves.

Acknowledgment. We thank Dr. M. Hashimoto, the Director of these Laboratories, for his encouragement throughout this work. Thanks are also due to Drs. T. Kadokawa, K. Hosoki, and K. Takeyama and Messrs. K. Nakatsuji and B. Fujitani for pharmacological assays and the staff of the Analytical Section of these Laboratories for the elemental analyses and spectral measurements.

(26) Available from Molecular Design Ltd., San Leandro, CA.
(27) Weiner, P. K.; Langridge, R.; Blaney, J. M.; Schaefer, R.; Kollman, P. A. *Proc. Natl. Acad. Sci. U.S.A.* **1982**, *79*, 3754.

Modeling Alcohol Metabolism with the DARC/CALPHI System

Christiane Mercier,* Véronique Fabart, Yves Sobel, and Jacques-Emile Dubois*

Institut de Topologie et de Dynamique des Systèmes de l'Université Paris 7, associé au C.N.R.S., 1 Rue Guy de la Brosse, 75005 Paris, France. *Received February 5, 1990*

We present our general system for QSAR search, CALPHI (Computer-Aided Law by Hyperstructure Investigation) set up in the context of the DARC structural language. We use it to construct global, fragmentary, and topological models of the capacity of alcohols to undergo glucuronidation. The DARC/PELCO model, more precisely and more significantly, explains 98% of the total variance with only three parameters, while treating the whole set of primary, secondary, and tertiary alcohols, whereas the best previously reported treatment restricted to primary alcohols, explains only 90% of the variance with two parameters. It provides an explicit and more precise interpretation of alcohol metabolism. The PELCO methodology is extended to evaluate the prediction reliability of both global and fragmentary models. PELCO leads to more predictions when comparison is made at the same level of reliability.

Introduction

It is generally agreed that aliphatic alcohols are metabolized and eliminated from the body by two main pathways, namely by in vivo oxidation to aldehydes, acids, ketones, and carbon dioxide or by conjugation with glucuronic acid to give highly water soluble glucoronides. It is worthwhile determining the factors which influence the path of elimination and to predict that chosen for a particular alcohol, for example in the field of detoxication studies. Thirty alcohols have been tested for their in vivo glucuronic acid conjugation capacity in rabbits.[1] Hansch et al.[2] correlated this activity with the partition coefficient, log *P*, and steric hindrance, E_s, but in two separate correlations for only some of the compounds. Furthermore, while these relationships allow one to evaluate the relative

(1) Kamil, J. A.; Smith, J. N.; Williams, R. T. *Biochem. J.* **1953**, *53*, 129.
(2) Hansch, C.; Lien, E. J.; Helmer, F. *Arch. Bioch. Biophys.* **1968**, *128*, 319.

0022-2623/91/1834-0934$02.50/0

influence of physicochemical parameters and their optimal values, their predictive capability is limited to those structures for which the external parameter values can be determined experimentally or by use of structure–property relationships.

In the field of computer-aided design, we have developed an interactive graphic system for predicting reactivity, physicochemical properties or biological activities of molecules, using their characteristic structural elements. Initially conceived to implement the DARC/PELCO topological method,[3] the CALPHI (Computer-Aided Law by Hyperstructure Investigation) system has been progressively optimized simultaneously with its use especially on biological activities. Its significant application on extended and complex populations[4-6] led us to develop new concepts.[7-9] Its success in rationalizing the planning of experiments in the search for more active and less toxic compounds in anticholinergic series[10] showed the efficiency of the DARC/PELCO methodology. Given the performance and the possibilities of systematic exploration of the CALPHI procedure, we wanted to make this tool more general by gradually encompassing most QSAR search methods.

After briefly describing the DARC/CALPHI SAR search procedure, we use it to construct predictive models for the glucuronide ability of alcohols. We then compare the results of the global, fragmentary and topological approaches as well as their interpretative and predictive power.

Method. DARC/CALPHI SAR Search Procedure

CALPHI is our general system for implementing the PELCO[11] methodology in a computer-assistance framework. It employs subsystems for structural data display, a hyperstructure space-builder program, and several modules for management, multiple regression analysis, and prediction of structure and property data. The originality of CALPHI lies in the communication language, which is based on the DARC ordered chromatic graph concept.[12] This very general yet refined concept makes several approaches possible by using either topological, fragmentary, or global variables.

The data are either extracted from a data bank[10] or directly acquired, as here, with an interactive graphic procedure in the classical language of the drawn developed formula for the structures. The experimental compounds are displayed as simplified ordered chromatic graphs[9] in which the geometrical positions of the atoms reflect the order induced by generation (Figure 1). They are ordered, one to each other, according to the induced order. The experimental population trace, automatically obtained by superimposition of the ordered chromatic graphs, constitutes a visual representation of the basic structural elements of the population (Figure 2).

By starting with these data, it is possible to create the multidimensional structural variable to be correlated by an interactive procedure. The topochromatic vectors, which form the basic structural variable in the DARC/PELCO method, are automatically constructed by choosing all the structural elements existing in the population trace. These vectors can be modified by extending or reducing the dimensions of the structural representation space.[9] The primary topochromatical sites s_p, which constitute the basic elements of this model, can be automatically or interactively combined into condensed sites s_c, interaction sites s_i or equivalent sites s_e. The resulting modulated vectors constitute a DARC/PELCO structural variable if the complex sites result from hypotheses deduced from the treatment. They generate fragmentary or global variables if they are made a priori.

The optimal DARC/PELCO correlation is sought according to defined criteria: precision and predictive and interpretative power. It is based on the detection of singularities and regularities, given experimental precision. The initial representation space, which contains all the elements of the trace, is progressively modulated by introducing complex sites up to the optimal representation space. Interaction sites s_i account for some additivity deviations while equivalence sites s_e reflect regularities. The resulting modulated trace constitutes the basis for calculating the optimal DARC/PELCO model. At each step, the user acquires new hypotheses, deduced from the previous treatment, and the new SAR is performed by multiple linear regression. A stepwise regression module is available to detect the significant parameters.

The DARC/GEANT hyperstructure space-builder program automatically constructs, numbers, and locates all the structures of the prediction range, called "proference".[3,5] The results of the optimal DARC/PELCO correlation are used to calculate the predicted values, and a specific module estimates their reliability.[8]

The modular nature of the DARC/CALPHI system and its organization around a pivot file, which contains all the information concerning a population, make it possible to add on new modules. Its implementation with a dynamic memory management makes it possible to treat a large number of structural and pharmacological data.

Experimental Population

The experimental population consists of 27 alcohols, whose structures and activity values appear in Figure 1. Of the 30 alcohols tested by Kamil et al.[1] for their in vivo glucuronic acid conjugation capacity, three cannot be used for data treatment. Methanol yields no glucuronide, and the absorption of 1-decanol and 1-octadecanol is incomplete. The activity is measured by using an index, MR, which is the molar rate of glucuronide formation with respect to the dose of alcohol injected into a rabbit's stomach. After determining the normal output of glucuronic acid, the extra glucuronic acid extracted for each alcohol was determined simultaneously on three animals by the naphthoresorcinol reaction with the photoelectric absorptiometer.[13] The activity variable, chosen for the

(3) Dubois, J. E.; Laurent, D.; Aranda, A. *J. Chim. Phys.* **1973**, *70*, 1608; 1616.
(4) Dubois, J. E.; Laurent, D.; Bost, P.; Chambaud, S.; Mercier, C. *Eur. J. Med. Chem.* **1976**, *11*, 225.
(5) Mercier, C.; Dubois, J. E. *Eur. J. Med. Chem.* **1978**, *14*, 415.
(6) Mercier, C.; Sobel, Y.; Dubois, J. E. *Eur. J. Med. Chem.* **1981**, *16*, 473.
(7) Dubois, J. E.; Mercier, C.; Sobel, Y. *C. R. Acad. Sci., Paris* **1979**, *289C*, 89.
(8) Dubois, J. E.; Sobel, Y.; Mercier, C. *C. R. Acad. Sci., Paris, Série II* **1981**, *292*, 783.
(9) Mercier, C.; Sobel, Y.; Dubois, J. E. *Ann. Math. Chem.* In press.
(10) Mercier, C.; Trouiller, G. In *Quantitative Structure–Activity Relationships in Drug Design*; Fauchère, J. L., Ed.; Alan R. Liss, Inc.: New York, 1989; p 203. Mercier, C.; Trouiller, G.; Dubois, J. E. *Quant. Struct.-Act. Rel.* **1990**, *9*, 88.
(11) Dubois, J. E.; Sobel, Y. *J. Chem. Inf. Comput. Sci.* **1985**, *25*, 326.
(12) Dubois, J. E. In *Computer Representation and Manipulation of Chemical Information*; Wipke, W. T., Heller, S., Fellmann, R., Hyde, E., Eds.; Wiley: New York, 1974; p 239. Dubois, J. E. *Isr. J. Chem.* **1975**, *14*, 17.
(13) Hanson, S. W. F.; Mills, G. T.; Williams, R. T. *Biochem. J.* **1944**, *38*, 274.

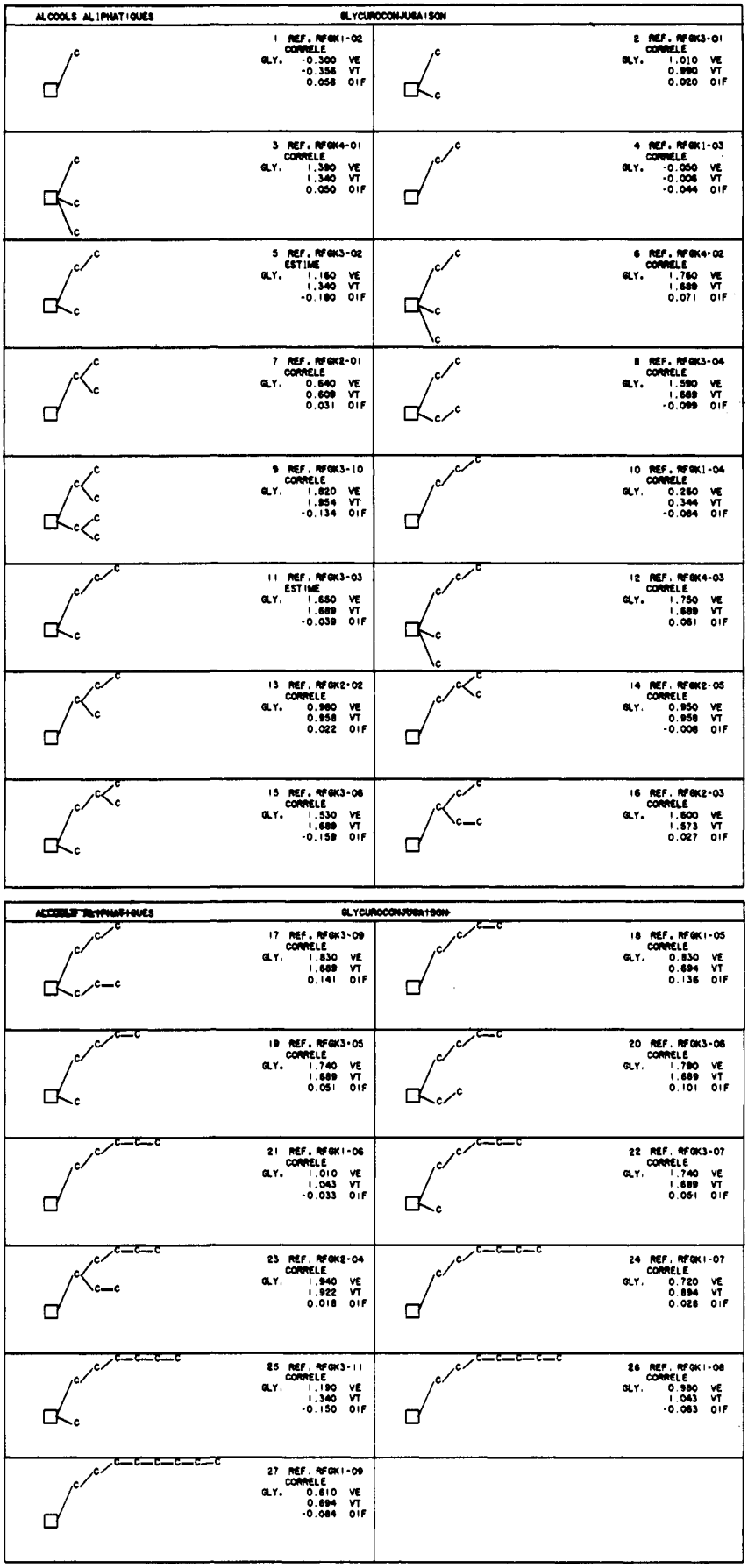

Figure 1. Glucuronic acid conjugation capacity of aliphatic alcohols. The 27 aliphatic alcohols are presented on this computer diagram as simplified ordered chromatic graphs. The square represents the focus, i.e. the C–OH group characterizing the series. The geometrical arrangement of the carbon atoms reflects the order induced over the environment. Primary, secondary, and tertiary alcohols have one, two, and three substituents issuing the focus, respectively. Coding associated with each structure is as follows: REF, reference numbers in (1); CORRELE, compounds included in the DARC/PELCO treatment; ESTIME, compounds belonging to the retrospective proference; VE, experimental values; VT, values calculated from the optimal DARC/PELCO relationship; DIF, difference between observed and calculated values.

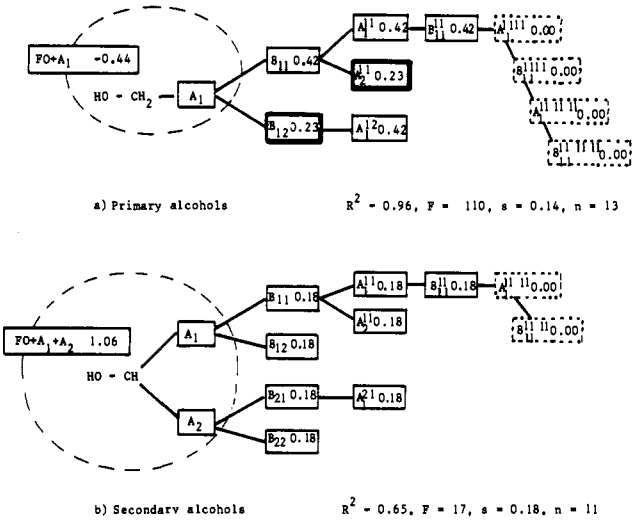

Figure 2. Global models. The two global models performed separately on primary and secondary alcohols can be expressed as (a) log MR = −0.44(±0.19) + 0.42(±0.07)$\sum l$ + 0.23(±0.16)$\sum b$ (1) and (b) log MR = 1.06(±0.26) + 0.18(±0.09)$\sum C$ (2), where $\sum l$ and $\sum b$ represent the number of chain lengthening and branching carbon atoms, $\sum C$ the number of carbon atoms, with a maximum lengthening of four carbon atoms ($l \leq 4$). The contributions of the carbon atoms are presented on the corresponding traces:

(a) ⋯⋯ Σl; ▭ Σb; (b) ▭ ΣC.

structure–activity correlations, is the logarithm of this index, i.e., log MR, whose average precision is 0.09 with a maximum deviation of 0.27.

Results

Hansch et al.[2] previously reported two separate correlations: A. The equation for primary alcohols versus partition coefficient and steric hindrance:

$$\log MR = -0.176\ (\log P)^2 + 0.806 \log P - 0.524\ E_s + 1.067$$

$$R^2 = 0.899,\ s = 0.169,\ n = 11$$

B. The equation for secondary alcohols versus partition coefficient only:

$$\log MR = -0.326(\log P)^2 + 1.444 \log P + 0.738$$

$$R^2 = 0.719,\ s = 0.174,\ n = 11$$

Most of the log P values were calculated by taking advantage of their additive constitutive nature. They were based on the experimentally determined values for methanol (−0.66), 2-butanol (0.61), 3-butanol (0.37), and *tert*-amyl alcohol (0.89). To these base values was added 0.50 for each chain-lengthening carbon and 0.30 for each branching carbon atom. It was then of interest to test directly the influence of the number of carbon atoms, lengthening or branching ones.

1. Global Models. A first correlation is carried out on the 27 primary, secondary, and tertiary alcohols with the number of carbon atoms $\sum$C taken as the structural variable, which amounts to treating all the sites in the trace as though they were equivalent. The statistical criteria ($R^2 = 0.24$, $F = 8$, $s = 0.53$) are very poor. These results lead us to test primary and secondary alcohols separately.

The regression performed on the 13 primary alcohols with again the number of carbon atoms, $\sum C$, taken as the structural variable, is slightly more significant ($R^2 = 0.44$, $F = 9$, $s = 0.47$).

The power of the DARC/CALPHI system and the fundamental character of the basic structural elements used enables one to refine this model. Major deviations between calculated and observed values occur for all compounds having more than four chain-lengthening atoms. As these suggest that the influence of chain lengthening raises a limit, we modified the $\sum C$ variable by eliminating the carbon atoms beyond the fourth lengthening site B_{11}^{11} (Figure 2). The regression obtained is much more significant ($R^2 = 0.93$, $F = 139$, $s = 0.17$) and confirms our hypothesis about the influence of chain lengthening. Nevertheless, as large deviations are observed for compounds having branching atoms, we break down the $\sum C$ variable into two structural variables: $\sum l$ ($l \leq 4$) for chain-lengthening atoms and $\sum b$ for branching atoms. The regression (Figure 2) carried out with these two new structural parameters is excellent:

$$\log MR = -0.44 + 0.42\sum l + 0.23\sum b \quad (1)$$

$$R^2 = 0.96,\ F = 110,\ s = 0.14,\ n = 13$$

The statistical criteria correspond to a <0.1% risk, and the precision (0.12) is the same as the experimental one.

The optimal correlation for the 11 secondary alcohols is performed in a similar way. In this case, only one structural variable is retained, the number of carbon atoms $\sum C$ with a limit for chain-lengthening atoms ($l \leq 4$). The correlation obtained (Figure 2):

$$\log MR = 1.06 + 0.18\sum C \quad (2)$$

$$R^2 = 0.65,\ F = 17,\ s = 0.18,\ n = 11$$

is poor, and the inaccuracy on the calculated values (0.16) is greater than for the observed values (0.06).

2. Fragmentary Models. The next study aims to check the additivity concept of the Free–Wilson model[14] and especially the equivalence hypothesis between substituents in symmetrical positions, advocated by Schaad.[15] This modified Free–Wilson model assumes that identical groups with the same origin make the same contributions, regardless of their occurrence.

The fragments methyl, ethyl, isopropyl, etc. are interactively constructed by grouping together their components into condensed sites, which appear as chromatic sites in the three positions A_1, A_2, and A_3 (Figure 3).

The modified Free–Wilson model which we call a nonordered fragmentary model is applied to the 27 alcohols by introducing the 13 substituent parameters, grouped in equivalence sites when appearing in several positions. The treatment provides the substituent activity contributions (eq 3, Figure 3) as well as the statistical criteria ($R^2 = 0.92$, $F = 12$, $s = 0.24$). Although this correlation is a good indication, important deviations are observed for compounds having one of the 4 substituents which appear simultaneously in several positions. This suggests that the influence of a substituent depends on its position in one of the three possible directions of development.

Again, the fundamental character of the structural variable used enables one to refine this model. The nonequivalence between substituents is taken into account by imposing an order on the substituents that is derived from knowledge of the topological order.

The resulting ordered fragmentary model is applied with 18 structural parameters corresponding to the different substituents in each direction. The statistical criteria (R^2

(14) Free, S. M.; Wilson, J. W. *J. Med. Chem.* **1964**, *7*, 395.
(15) Schaad, L. J.; Werner, R. H.; Dillon, L.; Field, L.; Tate, C. E. *J. Med. Chem.* **1975**, *18*, 344.

Table I. Site/Cosite Occurrence and Reliability Distribution in the Population Studied[a]

	sites															
sites	A_1	A_2	A_3	B_{11}	B_{12}	B_{21}	B_{22}	A_1^{11}	A_2^{11}	A_1^{12}	A_1^{21}	B_{11}^{11}	$A_1^{11\,11}$	$B_{11}^{11\,11}$	$A_1^{11\,11\,11}$	$B_1^{11\,11\,11}$
A_1	25	X	X	X	X	X	X	X	X	X	X	X	X	X	X	X
A_2		12	X	10	1	X	X	7	1	★	X	4	2	1	★★★	★★★
A_3			3	2	★	★	★★★	1	★★★	★★★	★★★	★★★	★★★	★★★	★★★	★★★
B_{11}				22	X	X	X	X	X	X	X	X	X	X	X	X
B_{12}					5	1	X	3	★★	X	★★★	1	1	★★★	★★★	★★★
B_{21}						4	X	2	★★★	★★★	X	1	★★★	★★★	★★★	★★★
B_{22}							1	★★★	★★★	★★★	★★★	★★★	★★★	★★★	★★★	★★★
A_1^{11}								17	X	X	X	X	X	X	X	X
A_2^{11}									2	★	★★★	★★	★★★	★★★	★★★	★★★
A_1^{12}										2	★★★	1	1	★★★	★★★	★★★
A_1^{21}											1	★★★	★★★	★★★	★★★	★★★
B_{11}^{11}												10	X	X	X	X
$A_1^{11\,11}$													7	X	X	X
$B_{11}^{11\,11}$														4	X	X
$A_1^{11\,11\,11}$															2	X
$B_{11}^{11\,11\,11}$																1

[a] The reliability of the perturbations associated with the binary cosites is ★★★★, if the cosite exists in the population, ★★★, if the cosite includes a site beyond the F_A frontier or a site s and a site beyond the inhibiting frontier F(s), ★★, if the cosite belongs to the active environment and does not correspond to the sixth structural modification for secondary and tertiary alcohols or to the seventh one for primary alcohols, and ★, if the cosite is required to specify one inhibiting frontier. A number indicates occurrence of tested sites (diagonal), and cosites (four-star reliability); X, implied cosites (necessarily present—occurrence the same as diagonal); ★, ★★, and ★★★, reliability of untested cosites.

= 0.94, F = 9, s = 0.24) are better, and the substituent activity contributions (eq 4, Figure 3) confirm the nonequivalence hypothesis.

3. DARC/PELCO Model. The 27 aliphatic alcohols, whose trace is represented in Figure 4, all have a common substructure: the focus of the description and site A_1. The secondary alcohols all have site A_2 and the tertiary alcohols site A_3 as well. The graphs of the minimal primary, secondary, and tertiary alcohols are as follows:

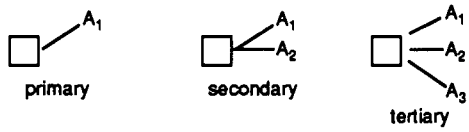

The experimental population to be treated is chosen so as to ensure a maximal structural interpolation of the predictive area.[5,9] The theoretical key population groups the minimal and maximal compounds associated with the sites of the trace.[3] Their structures are dark framed in Figure 5. The available key population includes the experimental compounds most resembling the theoretical key structures and contains 25 compounds marked "CORRELE" in Figure 1.

There are three steps in establishing the optimal topo-information relationship: exploratory correlation, detection of irregularities, and search for regularities.[9,16]

The exploratory correlation is carried out on the available key population with all the trace sites. The statistical criteria (R^2 = 0.96, F = 12, s = 0.22) are satisfactory since the F test shows that the correlation is significant with a <0.1% risk. However, the inaccuracy on the calculated values (0.13) is slightly greater than the observed experimental uncertainty (0.09). Major deviations are observed for compounds having an A_2 site. This suggests that some perturbations are nonadditive when A_2 site is occupied.

Deviations from additivity are taken into account by introducing interaction sites i.e. cosites which designate the simultaneous existence of two sites, each of which could exist without the other one.[7] Here, one of the sites is A_2, the other one is one of the seven sites (B_{11}, B_{12}, A_1^{11}, A_2^{11}, B_{11}^{11}, $A_1^{11\,11}$ or $B_{11}^{11\,11}$) (The sites are concentrically organized around the focus and successively called A_i and B_{ij}. The symbols of the successors issuing a B_{ij} site are marked with a superscript ij: A_2^{11} is issued from $B_{11}^{13,9}$) existing both without and with site A_2 in experimental key compounds (see row A_2 in Table I). The two cosites $A_2{*}A_2^{11}$ and $A_2{*}B_{11}^{11}$

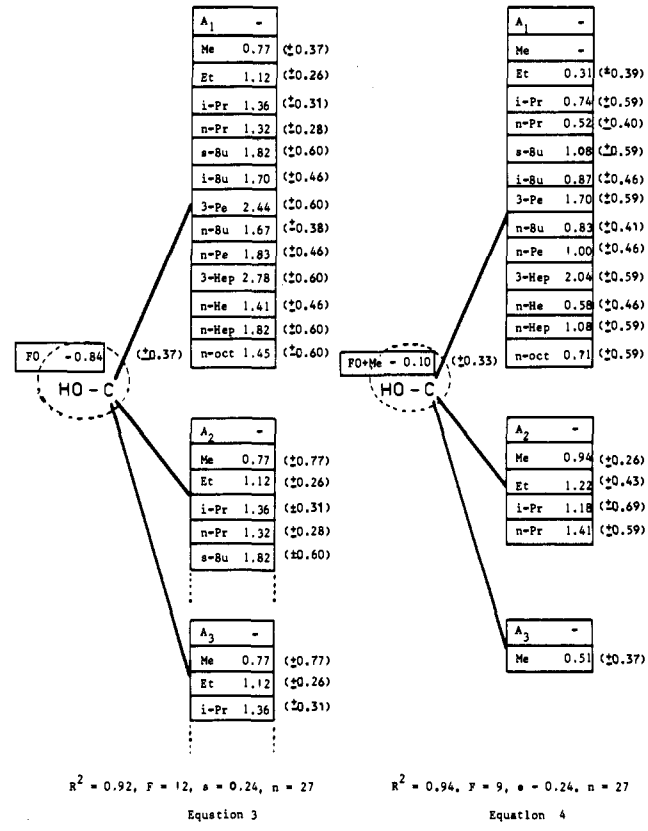

Figure 3. Nonordered and ordered fragmentary models. The substituent contributions to glucuronic acid conjugation are different in the three positions. The difference is about one logarithmic unit between the first and second positions for ethyl and *n*-propyl.

(16) Dubois, J. E.; Mercier, C.; Panaye, A. *Acta Pharm. Yugosl.* **1986**, *36*, 135.

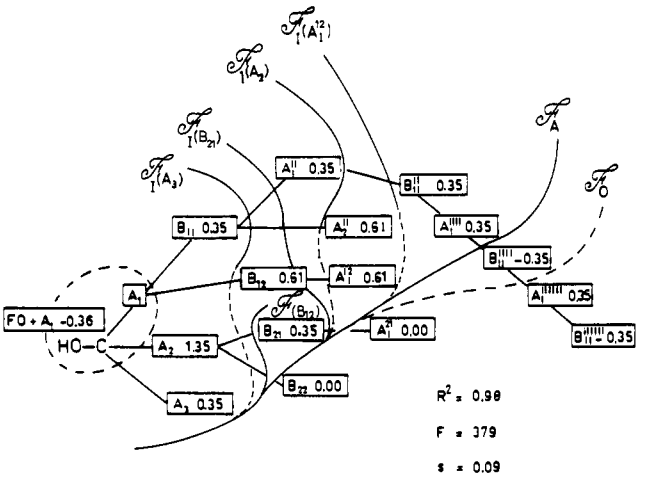

Figure 4. Optimal DARC/PELCO model. The relationship can be expressed as log MR = $-0.36(\pm0.11) + 1.35(\pm0.08)A_2 + 0.61(\pm0.06)\sum b + 0.35(\pm0.04)\sum l$, where $\sum b$ groups the branching sites and $\sum l$ the chain-lengthening sites. Sites beyond the activity frontier F_A have a zero or unfavorable influence. Sites beyond the inhibiting frontiers $F_I(s)$ have a zero influence in the presence of site s. — = established frontiers. --- = hypothetical frontiers.

are selected from the seven possible ones including A_2 by a stepwise regression. The correlation obtained is very good ($R^2 = 0.98$, $F = 23$, $s = 0.15$). The contributions, called the average perturbations $\bar{p}$, of the two cosites $A_2{}^*A_2^{11}$ and $A_2{}^*B_{11}^{11}$ are approximately the negative values of the respective contributions of A_2^{11} and B_{11}^{11}:

$$\bar{p}(A_2{}^*A_2^{11}) \approx \bar{p}(A_2^{11}) \qquad \bar{p}(A_2{}^*B_{11}^{11}) \approx \bar{p}(B_{11}^{11})$$

Thus, sites A_2^{11} and B_{11}^{11} have no effect when A_2 site is present, i.e. for secondary and a fortiori tertiary alcohols. Let us examine the minimum structural configurations compatible with these structural elements:

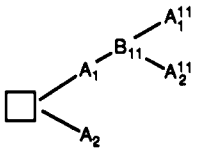

4-Me-2-pentanol

$A_2{}^*A_2^{11}$

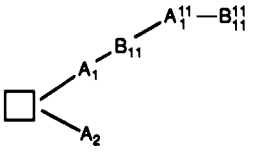

2-hexanol

$A_2{}^*B_{11}^{11}$

Those cosites correspond to the fifth carbon introduced into the environment. Thus, the results suggest that the fifth carbon has no effect for secondary and tertiary alcohols. The other cosites reflecting this hypothesis and existing in the experimental population are listed below:

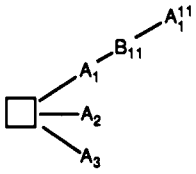

$A_3{}^*A_1^{11}$

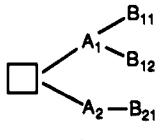

$B_{12}{}^*B_{21}$

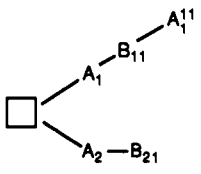

$B_{21}{}^*A_1^{11}$

For primary alcohols only the sixth chain-lengthening atom $B_{11}^{11\ 11}$ has no more positive influence: $\bar{p}(B_{11}^{11\ 11}) \approx -0.35$. Indeed, some oscillation is observed along with chain lengthening beyond the fifth atom. However, as this oscillation starts with a negative trend, no more increase of activity is observed (see contributions of sites after $A_{11}^{11\ 11}$, Figure 4). This leads us to test the cosite corresponding to the sixth carbon introduced:

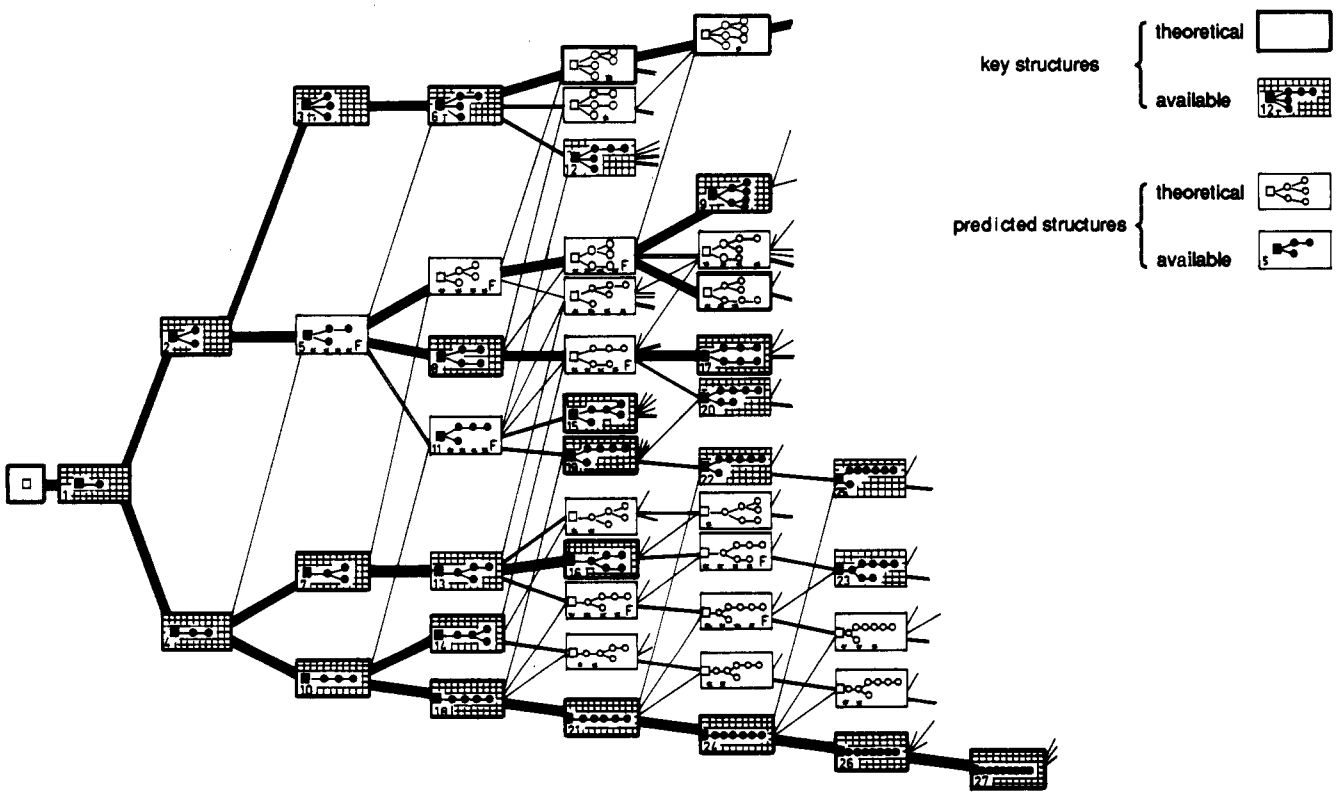

Figure 5. Hyperstructure weighted by prediction reliability. All the new structures (white background) generated from the experimental key structures (cross-hatched and dark framed) are predictable with minimal reliability. Structures marked F are predictable with maximal reliability. Intermediate reliabilities are determined at level 2 by examining, in each structure, the binary cosites controlling reliability.

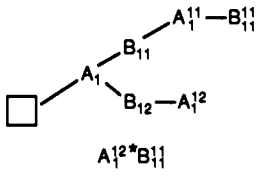

A_1^{12}*B_{11}^{11}

The introduction of the cosites reflecting these hypotheses leads to a very significant correlation ($R^2 = 0.99$, $F = 62$, $s = 0.09$). This relationship describes very precisely (±0.03) the dependence of glucuronic acid conjugation capacity on structure. However, the contributions of several sites are equivalent, within experimental precision (0.09), suggesting greater regularity.

Regularities are detected by introducing equivalence sites, which group sites with equal influence on property and belonging to homogeneous structural series, and eliminating the less significant parameters. Two main classes of homogeneous sites are detected:

A. Chain-lengthening sites A_3, B_{11}, B_{21} (in the absence of B_{12}), A_1^{11} (in the absence of A_3 or B_{21}), B_{11}^{11} (in the absence of A_2 or A_1^{12}), $A_1^{11\,11}$ (in the absence of A_2), $B_{11}^{11\,11}$, $A_1^{11\,1\,111}$, and $B_{11}^{11\,11\,11}$ grouped in the $\sum l$ variable.

B. Branching sites B_{12}, A_2^{11} (in the absence of A_2) and A_1^{12} grouped in the $\sum b$ variable.

Site A_2 remains individualized and sites B_{22} and A_1^{21} are not retained.

The optimal topo-information relationship

$$\log MR = -0.36 + 1.35A_2 + 0.35\sum l + 0.61\sum b$$

$$R^2 = 0.98,\ F = 379,\ s = 0.09,\ n = 25$$

describes glucuronic acid conjugation capacity as precisely as does experimental information.

The results are visualized on the trace of the population (Figure 4). The values inside each rectangle represent the contributions to activity of the corresponding sites s (A_2, A_3, etc.), called the average perturbations of information $\bar{p}$(s) ($\bar{p}(A_2)$, $\bar{p}(A_3)$, etc.).

Discussion

The statistical criteria (Table II) indicate that the DARC/PELCO model is the most significant with a precision close to experiments. It explains 98% of the total variance with only three parameters while treating the whole set of compounds. The fragmentary models (eqs 3 and 4) explain 92% and 94% of the total variance but with 13 and 17 parameters, respectively. The global models (eqs 1 and 2) explain 96% of the variance for primary alcohols and only 65% for secondary ones. The Hansch model is less significant than the global one for primary alcohols and slightly better for secondary ones.

1. Interpretation. Interpretation of the results is easier for global models, more precise with the DARC/PELCO method, and difficult with fragmentary models because, in this last case, the results do not allow us to deduce a general law.

Analysis of eq 1 and 2 for global models shows that the glucuronic acid conjugation of primary alcohols is enhanced by chain lengthening, with a maximum for 1-pentanol, and by branching. For secondary alcohols, it is only enhanced by the number of carbon atoms with a maximum for 4-octanol. This interpretation is similar to Hansch's, if we consider that the influence of the number of carbon atoms, especially those corresponding to chain lengthening, is taken into account by the partition coefficient and that of branching atoms by the E_s steric parameter. Indeed, for these authors, glucuronic acid conjugation depends mainly on the partition coefficient with an ideal log P_o of 2.29 for primary alcohols and 1.75 for secondary. It is enhanced by steric hindrance in the case of the primary alcohols but is practically insensitive to this factor in the case of secondary ones.

In the DARC/PELCO method, the results are first analyzed locally to specify the influence of structural modifications on activity, then globally, revealing several frontiers of influence on activity.

The sites are grouped in four classes depending on their contribution (Figure 4):

A. Site A_2 has a major contribution, +1.35; it accounts for the differences in behavior of (i) primary alcohols and (ii) secondary and tertiary ones.

B. Branching sites have an important contribution, +0.61.

C. Chain-lengthening sites have a slight influence, 0.35, which increases activity up to $A_1^{11\,11}$ and then decreases and oscillates.

D. Sites B_{22} and A_1^{21} have no effect.

Among the favorable branching and chain-lengthening sites, many have no effect in the presence of other sites:

A. Branching sites. A_2^{11} has no effect in the presence of site A_2, i.e. for secondary and a fortiori tertiary alcohols.

B. Chain-lengthening sites. $A_1^{11\,11}$ has no effect in the presence of A_2 (i.e. for secondary alcohols), B_{11}^{11} in the presence of A_2 or A_1^{12} (for secondary and α-Et branched alcohols), A_1^{11} in the presence of A_3 or B_{21} (for tertiary or 3-secondary alcohols) and B_{21} in the presence of B_{12} (for α-Me branched alcohols).

Thus the glucuronic acid conjugation capacity depends on three factors:

A. The nature of the hydroxyl group. Secondary and tertiary alcohols are of comparable activity. They are both strongly glucuronidated, approximately 10 times better than the isomeric primary alcohols. This is evidenced by a very much larger contribution of site A_2 (1.35) with respect to chain-lengthening $\sum l$ (0.35).

B. Branching. Primary alcohols are very sensitive to branching which greatly increases their glucuronidation capacity. With secondary and tertiary alcohols, saturation appears for β branching and for a second α branching.

C. Chain lengthening. In all three groups of alcohols, the chain lengthening increases glucuronidation and reaches a saturation threshold corresponding to an alcohol having six carbon atoms if the function is primary and five carbon atoms otherwise.

This analysis provides an explicit and more precise interpretation of alcohol metabolism. Elimination of a given alcohol depends mainly on the number of carbon atoms, the nature of the hydroxyl group and the extent of carbon chain branching. For Kamil et al.,[1] the general conjugation order of aliphatic alcohols is tertiary > secondary > primary and, since oxidation goes contrary-wise, they conclude that the unoxidized portion of the alcohol is subjected to glucuronidation. The results here class secondary alcohols with tertiary ones, which agrees with the fact that ketones can give glucuronides. Moreover, since the steric effect seems more important for primary alcohols and inhibits their oxidation, we can conclude, in agreement with Hansch,[2] that steric hindrance increases the glucuronidation of primary alcohols by inhibiting their oxidation.

Global analysis is facilitated by the detection of several structural influence frontiers (Figure 4):

A. An activity frontier F_A, beyond which sites either do not effect or decrease activity;

B. Five inhibiting frontiers $F_I(A_2)$, $F_I(A_3)$, $F_I(B_{12})$, $F_I(B_{21})$, and $F_I(A_1^{12})$ beyond which sites have no effect when

Table II. Statistical Criteria for the Correlations Carried Out by the Global (1) and (2), Fragmentary (3) and (4), and DARC/PELCO (5) Methods[a]

method	global (1)	global (2)	fragmentary non-ordered (3)	fragmentary ordered (4)	DARC/PELCO (5)
P_{exp}					
alcohols	primary	secondary	primary, secondary, and tertiary		
number	13	11	27	27	25
precision	0.12	0.06	0.09	0.09	0.09
retrospective proference	0	0	0	0	2
number of parameters	2	1	13	17	3
R^2	0.96	0.65	0.92	0.94	0.98
F global	110	17	12	9	379
	0.001	0.01	0.001	0.001	0.001
standard deviation	0.14	0.18	0.24	0.24	0.09
average deviation	0.12	0.16	0.16	0.14	0.08

[a] The retrospective proference includes the experimental compounds, which are not necessary to establish the relationship. These compounds make it possible to check the predictive capacity of the regression.

Table III. Extent and Reliability of the Predictions[a]

method	global		fragmentary		topological	
			ordered	nonordered	ordered: DARC/PELCO	nonordered
$P_{treated}$	primary alcohols	secondary alcohols			primary, secondary, and tertiary alcohols	
	13	11	27	27	25	27
predictions						
number	26	60	90	337 → 90 F min; 247 risky	339 → 8 F max; 331 F Min; 13 F_2^{****}; 51 F_2^{***}; 61 F_2^{**}; 214 F_2^{*}	11 453 risky → 338 F min; 11 115 risky
reliability	F_{min}	F_{min}	F_{min}	risky	F_{min}	risky

[a] Topology leads to a greater number of predictions than does cutting up molecules into fragments, for the same level of reliability. DARC/PELCO predictions are then organized in proferences of increasing reliability.

the site in question is occupied.

The frontiers are constructed by surrounding the sites favorable to activity. The activity frontier F_A, which is only valid for primary not α-Et branched alcohols, progressively comes closer to the focus with the extent of branching and the nature of the hydroxyl group. The inhibiting frontiers correspond to an activity frontier for α-Et branched primary alcohols ($F_I(A_1^{12})$), secondary alcohols in position 2 ($F_I(A_2)$) or 3 ($F_I(B_{21})$), tertiary alcohols ($F_I(A_3)$), and α-branched 3-secondary alcohols ($F_I(B_{12})$). These frontiers reflect the fact that the fifth carbon introduced into the environment for secondary and tertiary alcohols and the sixth carbon for primary alcohols have no effect. The established frontiers are extrapolated according to this fact and the corresponding hypothetical frontiers are represented by dashed lines in Figure 4.

In this study, the aim of which is to find a prediction law, it would be very interesting to localize a zero influence frontier F_0 beyond which sites have no effect. This appears to be beyond site B_{21} and $B_{11}^{11\,11}$. Indeed, sites B_{22} and A_1^{21} have no influence and the contribution of the last chain-lengthening sites oscillates slightly around zero with an amplitude of 0.35 close to the maximal experimental deviation (0.29). The hypothesis in favor of this F_0 frontier is confirmed by the experimentally determined value of 0.54 for 1-decanol, not included in this treatment.

This global analysis is used to estimate the reliability of the predictions.

2. Predictive Power. To compare the predictive ability of the four methods, we shall use the DARC/PELCO tools: proference, PR, which is equal to the number of structures generated from the studied population but which do not belong to it,[3,5] and pseudoproference, ψPR, which is equal to the number of structures generated on an enlarged trace of the studied population but which do not belong to the proference.[7]

Prediction reliability is measured by applying two interpolation criteria on a two-dimensional scale[8] and is expressed by an index F_k^j. Level k, from 1 to n, indicates the complexity of the sites taken into account in estimating reliability. Degree j, from one to four star, indicates the reliability of the perturbations associated with each site. It is maximal, four star, if the site (primary site or level 1 site, binary interaction site or level 2 site, etc.) exists in at least one structure of the experimental key population P. It is three star or two star if the estimation is based on hypotheses deduced from the treatment, and one star if the estimation is based on an a priori hypothesis. The predicted activity value of a structure is four star at level 2 only if all its sites and binary cosites have a four-star reliability.

For global models, the prediction ranges are proferences including 26 primary alcohols for equation 1 and 60 secondary alcohols for equation 2. These predictions all have four-star reliability at level 1, i.e. they only contain primary sites existing in the populations studied (Table III).

The ordered fragmentary model leads to a four-star, level 1 proference including 90 structures which constitute a part of the DARC/PELCO proference. The nonordered fragmentary model leads to 337 predictions of which 90 belong to proference and 247 to pseudoproference (Table III). The proference structures are identical with those of the ordered model, but the predicted values are less precise. The predictions of the pseudoproference area are risky because the equivalence hypothesis is not verified. They fall into the one-star, level 1 pseudoproference, which is the least reliable one. Thus, most of the predicted activities are >2, which corresponds to an MR > 100%; for

example, the compound predicted to be most active is tri(3-heptyl)methanol with a value of 7.50.

The DARC/PELCO proference includes 339 structures, which are located in the hyperstructure with respect to the experimental structures (Figure 5). Retrospective proference includes two structures, 5 and 11, not used for establishing the correlation. Their predicted values agree with those observed (Figure 1).

All the structures of the proference are predictable with a minimal reliability, four star at level 1, PR_{min} = 339. Since the available key population is not the theoretical one, this proference is completely reliable for only eight structures, PR_{max} = 8 (Figure 5).

Among the intermediate proferences, only those at level 2 are determined here (Figure 5). For each structure, the degree of reliability is automatically determined by considering the reliability degrees of the perturbations associated with its binary cosites (Table I). They are maximal, four star, if the cosites exist in the treated population. Untested binary cosites are considered to be zero with three-star reliability, if they include a site situated beyond the activity frontier F_A or a site s and a site beyond the inhibiting frontier $F_I(s)$. They are considered to be zero with two-star reliability, if they include sites belonging to the active environment and are not required to specify the inhibiting frontiers. They are considered to be the negative value of the sixth or fifth carbon with one-star reliability when introduced in primary or secondary and tertiary alcohols, respectively. Grouping structures whose activity prediction is carried out with similar reliability leads to four level 2 reliability areas (Table III).

The predictive capacity of the DARC/PELCO method is thus both more reliable and more extensive than that of fragmentary models. Topology leads to a greater number of predictions than does cutting up molecules into fragments (Table I). For nonordered models, the number of predictions is 11 453 (11 480 - 27), if the description is topological, and only 337, if the description is fragmentary. Such predictions are risky because the equivalence hypothesis is not verified. For ordered models, the predictive capacity is 340, if it is a topological one, and 91 if it is a fragmentary one. Moreover, the DARC/PELCO method allows one to isolate, within the set of predictions, those which are reliable.

The power of the DARC/CALPHI system and the fundamental character of the structural variable, pertaining to ordered topological sites, enable one to express nuances for global, fragmentary or topological methods. Its use in constructing topohydrophobic or electronic models will be presented in a forthcoming paper.

Registry No. 1, 64-17-5; 2, 67-63-0; 3, 75-65-0; 4, 71-23-8; 5, 78-92-2; 6, 75-85-4; 7, 78-83-1; 8, 584-02-1; 9, 600-36-2; 10, 71-36-3; 11, 6032-29-7; 12, 590-36-3; 13, 137-32-6; 14, 123-51-3; 15, 108-11-2; 16, 97-95-0; 17, 589-55-9; 18, 71-41-0; 19, 626-93-7; 20, 589-82-2; 21, 111-27-3; 22, 543-49-7; 23, 104-76-7; 24, 111-70-6; 25, 123-96-6; 26, 111-87-5; 27, 143-08-8.

Specific Bradycardic Agents. 2. Heteroaromatic Modifications in the Side Chain of Specific Bradycardic Benzazepinones: Chemistry, Pharmacology, and Structure-Activity Relationships

Andreas Bomhard,*,† Manfred Reiffen,† Joachim Heider,† Manfred Psiorz,† and Christian Lillie‡

Department of Chemical Research, Dr. Karl Thomae GmbH, Postfach 1755, D-7950 Biberach 1, Germany, and Department of Pharmacology, Ernst-Boehringer Institut für Arzneimittelforschung, Dr. Boehringer-Gasse 5-11, A-1121 Wien, Austria.
Received July 2, 1990

Compound 1 (UL-FS 49) has recently been described as the representative of a novel class of antiischemic compounds termed "specific bradycardic agents". In search of specific bradycardic agents with different pharmacokinetic profiles, heteroaromatic analogues of 1 have been synthesized and evaluated for their bradycardic activity, selectivity, and duration of action. The chain length *n* and the nature of the heteroaromatic system of compounds 2 strongly determine the biological activities. Unsubstituted benzothiophenes and benzofurans in combination with a chain length of *n* = 2 give the most active bradycardic compounds. Some of the new compounds combine high bradycardic potency and selectivity with a short duration of action and may thus be useful for the development of short-acting specific bradycardic drugs.

The prevention of myocardial hypoxia by reducing the cardiac oxygen consumption is one of the main principles in the treatment of coronary heart disease.[1] Whereas this can be achieved by the administration of cardiodepressive agents like β-adrenoceptor antagonists[2,3] or calcium channel blockers,[4] these drugs may exert detrimental negative inotropic and hypotensive effects. Therefore a specific reduction of sinus heart rate, which is a major determinant of myocardial oxygen demand,[5] appears to be a desirable therapeutic approach.

Compound 1 has recently been described as the representative of a novel pharmacological class termed "specific bradycardic agents".[6-8] It reduces heart rate without concomitant negative inotropic or hypotensive effects.[9] Searching for potential follow-up compounds of 1, we directed our attention not only to agents with high activity

† Dr. Karl Thomae GmbH.
‡ Ernst-Boehringer Institut für Arzneimittelforschung.

(1) Sonnenblick, E. H.; Skelton, C. L. *Mod. Concepts Cardiovasc. Dis.* 1971, *40*, 9.
(2) Conolly, M. E.; Kersting, F.; Dollery, C. T. *Prog. Cardiovasc. Dis.* 1976, *19*, 203.
(3) Warltier, D. C.; Gross, G. J.; Jesmok, G. J.; Brooks, H. L.; Hardman, H. F. *Cardiology* 1980, *66*, 133.
(4) Meils, C. M.; Gross, G. J.; Brooks, H. L.; Warltier, D. C. *Cardiology* 1981, *68*, 146.
(5) Sonnenblick, E. H.; Ross, J., Jr.; Braunwald, E. *Am. J. Cardiol.* 1968, *32*, 328.
(6) Kobinger, W.; Lillie, C. *Eur. J. Pharmacol.* 1984, *104*, 9.
(7) Kobinger, W.; Lillie, C. *Eur. Heart J.* 1987, *8 (Suppl. L)*, 7.
(8) *Drugs Future* 1985, *10*, 639; (updates) 1986, *11*, 718; 1987, *12*, 825; 1988, *13*, 804.
(9) Franke, H.; Su, C. A. P. F.; Schumacher, K.; Seiberling, M. *Eur. Heart J.* 1987, *8 (Suppl. L)*, 91.

0022-2623/91/1834-0942$02.50/0